Elinvo (Electronics, Informatics, and Vocational Education)
Vol 11, No. 1, 2026, pp. 43-54
ISSN 2580-6424 (printed) | ISSN 2477-2399 (online)

Uncertainty Analysis of Roughness Profile Measurement Using the 6 Lighting Stereophotometry Method

Irawati Dewi Syahwir [*], Irwan Setiawan [2], Inayah Dwi Khaira [1]

[1]Academy of Metrology and Instrumentation, Sumedang, Indonesia
[2]Ministry of Trade, Bandung, Indonesia
[1] irawatidewisyahwir@gmail.com*; [2] irones46@gmail.com; [3] inayahdwikhaira@gmail.com
* corresponding author

Article Info

Article history:
Received October 27, 2025
Revised May 10, 2026
Accepted May 25, 2026
Available Online 30, 2026

Keywords:
Gauge Block, Surface Roughness, Photometric Stereo, Measurement Uncertainty, Six Light Sources.

Abstract

Surface roughness characterization of gauge blocks is a critical aspect of dimensional metrology for ensuring calibration accuracy. Conventional contact-based measurements risk inducing material surface wear; hence, a precise, non-contact alternative is highly required. This study proposes a non-contact surface roughness measurement system for stainless steel standards and gauge blocks. The system utilizes computer vision-based stereophotometry equipped with an innovative six-source radial illumination configuration. This six-light design aims to overcome shadow distortion constraints while increasing the mathematical data redundancy necessary for accurate surface topography reconstruction. The study was conducted on ten steel gauge block samples for both Class 0 and Class 1 grades, with a nominal range of 1.01 mm to 1.10 mm. The experimental results show that the system can measure the average roughness Ra in the range of 1.5712 µm to 2.1994 µm for Class 0, and 2.1644 µm to 2.7875 µm for Class 1. A comprehensive uncertainty analysis was performed, incorporating a rectangular distribution for camera resolution and a triangular distribution for temperature fluctuations. The metrological evaluation yields a consistent expanded uncertainty of 0.08 μm at a 95% confidence level (k=2). These findings confirm that the six-light configuration significantly enhances the reliability of the contactless measurement system, offering strong potential for precision inspection in the automotive and advanced manufacturing industries.

INTRODUCTION

The manufacturing industry relies heavily on quality control to regulate production and address precision issues, which traditionally has been performed through manual visual inspection [1]. In dimensional metrology, maintaining the surface quality of critical reference components—such as gauge blocks—is paramount [5]. Conventionally, surface roughness measurements have mostly utilized contact-based stylus instruments [2]. However, this approach risks inducing material surface wear, scratching the calibrated specimen, and suffers from slow data collection while struggling to reach complex micro-features [2, 6]. Consequently, advanced metrology is moving toward high-precision, contactless alternatives to eliminate physical wear and minimize measurement uncertainty [6].

To address these limitations, optical non-contact methods have been widely explored, particularly stereophotometry (photometric stereo) [2, 7]. This computer vision technique recovers the three-dimensional surface orientation and depth information of an object by capturing multiple images under varying lighting conditions [2, 5]. Prior research has successfully applied stereophotometry using three

ISSN 2580-6424 (printed) | ISSN 2477-2399 (online)

distinct lighting modes to inspect textures and estimate roughness, demonstrating superior non-destructive performance compared to traditional stylus contact methods [2, 8].

Despite these advancements, research specifically addressing the characterization of gauge block surface profiles remains highly limited, as most previous studies focused solely on dimensional calibration without considering micro-topographical details [7, 8]. Furthermore, conventional optical configurations with limited light sources often suffer from spatial occlusion and shadow distortion when capturing microprofiles, which skews the average roughness Ra values.

To overcome these constraints, this study proposes a novel non-contact optical metrology framework utilizing a computer vision-based stereophotometry method equipped with an innovative six-source radial illumination configuration. This design expands illumination coverage and increases the mathematical data redundancy necessary for precise surface topography reconstruction, thereby minimizing spatial artifacts and reducing shadow distortion

The primary objective of this research is to evaluate the measurement errors and uncertainties of the proposed system using high-resolution image processing on standard gauge blocks across Class 0 and Class 1 grades. The main contribution of this work lies in the implementation of a robust, stable, and low-deviation configuration that enhances the reliability of surface roughness profiling for primary dimensional standards. Ultimately, this framework provides a highly precise and non-destructive inspection alternative tailored for advanced manufacturing and high-precision industries.

METHODS

Stereophotometry Method

The reflection of light on an object can be measured when the incident light has a constant direction and intensity. Intensity can be determined by capturing several images of the object illuminated by light. The roughness of an object's surface can be determined by the diffuse reflection of light in all directions.

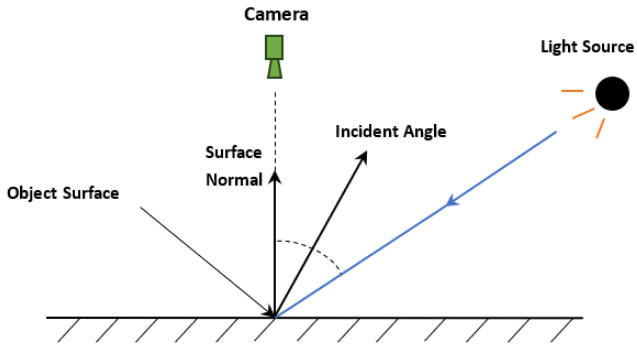

Figure 1. Photometric Stereo System

The method used is an image-acquisition system that obtains surface topography by varying the lighting. The image setup is shown in Figure 1. Figure 1(a) shows the light source system, which consists of six and twelve light sources in the form of LEDs (light emitting diodes) of the Cree type with a power of 1 watt and a tilt angle (α) between LEDs of 60° for 6 lighting [9]. The light sources are set to light up alternately with an intensity of about 18 cd, and the tilt angle (θ) is chosen to be about 55° [9][10], as shown in Figure 1(b).

The surface roughness parameter employed in this study is the arithmetic mean of the surface profile (Ra). Ra represents the arithmetic mean of the absolute values of the roughness heights relative to the measured average values. The mathematical expression is as follows equation 1:

$$R_a = \frac{1}{N}\sum_{i=1}^{n}\lfloor Z_i \rfloor \quad \ldots\ldots\ldots\ldots\ldots\ldots\ldots\ldots\ldots\ldots\ldots\ldots\ldots\ldots\ldots\ldots\ldots\ldots\ldots\ldots\ldots\ldots\ldots\ldots\ldots\ldots \quad (1)$$

ISSN 2580-6424 (printed) | ISSN 2477-2399 (online)

Where Ra is the average roughness height, N represents the number of measured points in the sample. The value of Ra is derived from the average height [12].

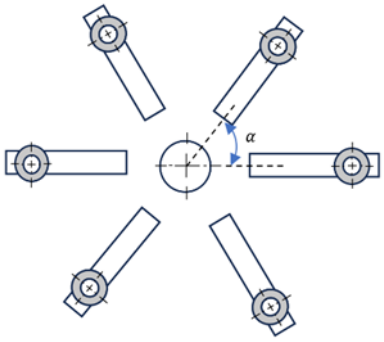

Figure 2. Image Acquisition System for Gauge Block Samples with 6 illuminations

The stereophotometry method in Figure 2 is a technique used to assess the shape and reflectance properties of an object to reconstruct its 3D geometry [28]. This method utilises light variations to assess surface gradients, which are determined based on a series of straight surfaces. Thus, surface gradients can be inferred from these measurements. Surface texture can be analysed using the obtained depth information [12][13].

The hardware design of this system integrates six light sources arranged symmetrically around the camera's optical axis, each with a controlled elevation angle. The technical justification for selecting these six light sources is based on minimising the least-squares error in the Photometric Stereo algorithm. With six different lighting angles, the system can minimise the effect of specular highlights on the gauge block's reflective surface. Methodologically, this configuration ensures that every surface slope gradient is captured through variations in light intensity, thereby improving the signal-to-noise ratio (SNR) of the acquired digital image.

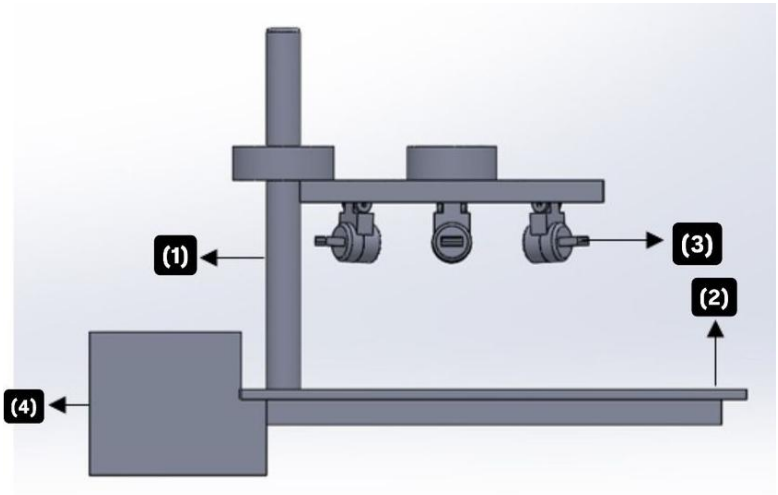

(1) Prototype Base Frame/ Foundation; (2) Base Table to House the Gauge Block; (3) 6 1-watt USB LED lights; and (4) Component Box.

Figure 3. Image Recording Device View

Figure 3 shows a mechanical system designed as part of the development of a gauge block surface roughness measurement instrument based on the stereo photometry method. This system consists of two main structures: a lower base for mounting the measuring object (the gauge block) and an upper base that supports the camera and lighting system. This structure is supported by a vertical support rod and a height-adjustable clamp. The camera used is a smartphone mounted perpendicular to the object. The

lighting system consists of six LED lights, with a 60 an angle between the light sources, and each LED is installed at an angle of approximately 55° to the object surface to produce lighting from different directions (multi-directional lighting).

To evaluate surface roughness, the reconstruction analysis averages the vertical gradients between surface peaks and valleys, enabling the classification of the gauge block against established reference standards [30]. The image processing pipeline begins with a masking operation to pinpoint specific target areas. By ignoring irrelevant background elements and noise generated by extreme light reflections, the mask confines the valid computational area strictly to the centre of the object's surface. Crucially, this masking framework computes the light direction vector across its three-dimensional spatial components (x, y, z). Based on these calibrated coordinates, the light direction vector at the calculated position is formalized through the equation 2:

$$\sqrt{x^2 + y^2 + z^2} \approx 1 \qquad \text{.....} \quad (2)$$

The vision-based data acquisition system utilized an integrated smartphone camera from an Apple Iphone 12. The primary wide-angle camera features a 12 MP image sensor resolution, a physical focal length of 4.2 mm (equivalent to 26 mm in a 35mm format), a wide aperture of f/1.6, and a pixel size of 1.4 µm. The optical lens configuration consists of a custom 7-element lens assembly. During the experiment, the camera's digital zoom function was completely disabled (maintained at 1x optical baseline) and the built-in autofocus mechanism was systematically locked to ensure a constant focal plane across all shots.

The camera was securely mounted at a fixed working distance of 120 mm, positioned perfectly perpendicular relative to the gauge block's flat surface. Because a specialized telecentric lens was not used in this experimental setup, perspective distortion was mathematically minimized and controlled by maintaining a rigid, fixed camera position, strict perpendicular mechanical alignment, and ensuring a constant working distance throughout the entire measurement cycle.

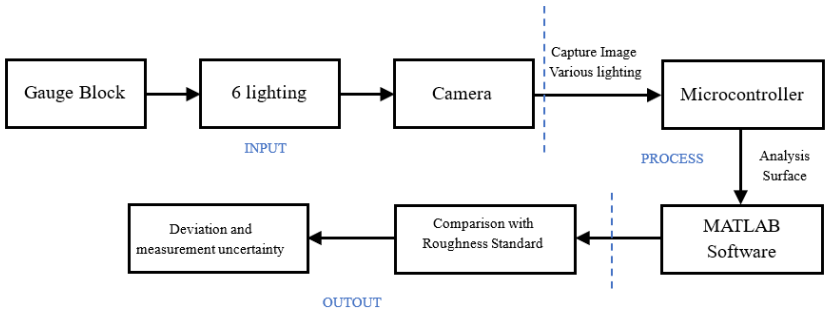

Figure 4. Diagram Block System Reconstruction Roughness Gauge Block with 6 lighting

After capturing the images, a systematic image preprocessing workflow was implemented in MATLAB to optimize the input data before executing the photometric stereo algorithm. The step-by-step workflow from raw image acquisition to the final surface reconstruction is detailed as follows:

1. Raw Image Acquisition and LED Calibration: The process initiated by capturing six raw images of the gauge block sample under six different directional LED light sources, which were controlled sequentially by the microcontroller. Prior to image acquisition, the six LEDs were rigorously tested to ensure stable and uniform illumination. Each LED shares identical rated power and nominal intensity specifications and was operated using a constant current driver circuit to prevent intensity fluctuations. Before starting the experiment, each LED was turned on individually and allowed to stabilize for a designated period to minimize thermal drift. The light intensity was verified using a digital lux meter to ensure that any residual brightness

ISSN 2580-6424 (printed) | ISSN 2477-2399 (online)

differences between the LEDs were negligible. The captured images were subsequently processed using calibrated light source direction vectors to maintain measurement integrity.

2. Color Space and Color Depth Conversion: The raw images captured by the camera were originally stored in the RGB color space with a depth of 8-bit per channel, resulting in 24-bit color images. These images were saved in PNG format. Prior to processing, the RGB images were converted into 8-bit grayscale images. This conversion is essential as the photometric stereo algorithm utilizes pixel intensity (luminance) matrices rather than color information to accurately reconstruct the surface profile.
3. Region of Interest (ROI) Cropping: A manual cropping operation was applied to isolate the specific target area of the gauge block from the background. This stage discards irrelevant background information and limits the computational domain strictly to the center of the object's surface.
4. Image Alignment: Coordinate alignment was performed across all six captured images from the different lighting angles to ensure perfect spatial registration and counteract any sub-pixel frame shifts or ambient vibrations during the experiment.
5. Intensity Normalization and Ambient Light Control: To minimize the influence of ambient light, the image acquisition process was strictly conducted inside a closed measurement chamber (dark-room environment). During image capture, all external light sources were completely blocked, and the ambient laboratory lighting was turned off. This setup ensures that the only active illumination originates from the controlled six-LED light system, meaning that any pixel intensity variations captured by the camera are solely caused by the changing directions of the six lamps. Additionally, a dedicated background masking was integrated to eliminate residual extreme reflections on the reflective steel surface.
6. Final Processing: The finalized, aligned, and masked grayscale matrices from the six lighting directions were then exported to the main photometric stereo function (unbiased_ps_directional) in MATLAB to calculate the surface normal and extract the arithmetic mean roughness (Ra).

The calculation of the uncertainty of the gauge block surface roughness profile measurement using the stereophotometry method with a fixed camera and 6 LED light sources positioned at specific angles around the gauge block. The working principle of this research is shown in the block diagram in Figure 4.

Roughness parameters are defined by various standards and selected according to the applied standards [101]. It is expressed in the parameter Ra (Mean Roughness), which is the arithmetic mean of the deviations of the surface profile from the mean centerline.

A gauge block, as shown in Figure 5, is a rectangular tool made of wear-resistant material with two flat surfaces, each with a parallel measuring surface. It can be used to connect the measuring surfaces of other gauge blocks to form composite assemblies or to longer measuring surfaces. This gauge block serves as a standard for calibrating dimensional measurements. The evaluation was performed using a standard Mitutoyo rectangular steel gauge block set conforming to ISO 3650, utilizing Class 0 and Class 1 grades to evaluate the photometric system's robustness against subtle differences in surface quality and reflectivity

ISSN 2580-6424 (printed) | ISSN 2477-2399 (online)

Figure 5. Gauge Block

The camera specifications used are 12 MP pixels, 2x optical zoom and up to 5x digital zoom, have 7 main element lenses and 100% Focus pixels.

Uncertainty Of Gauge Block Surface Roughness Measurement

The measurement uncertainty analysis for the gauge block surface roughness involves both Type A and Type B evaluations. Type A uncertainty is determined from repeated experimental trials modeled by a normal distribution. Type B uncertainty accounts for instrumental limitations, including camera resolution (rectangular distribution) and ambient temperature variations monitored via an analog thermometer (triangular distribution). Each uncertainty will be calculated using a combined uncertainty with a normal distribution (equation 3)

$$U_c = \sqrt{(U_1 \times C_1)^2 + (U_2 \times C_2)^2 + \cdots + (U_n \times C_n)^2} \quad \text{..... (3)}$$

where Uc is the combined uncertainty, C is the sensitivity coefficient, and Uexp is the uncertainty expanded with k=2 with a 95% confidence level. In equation 4 is the equation for calculating expanded uncertainty (Uexp)

$$U_{exp} = k \times U_c \quad \text{..... (4)}$$

All uncertainty components are systematically integrated to ensure the reliability of the measurement results. Type A uncertainty represents random variations from repeated testing, while Type B includes technical limitations of the instrument such as camera resolution and ambient temperature fluctuations. Combining these two types is done using the root-sum-square method according to Equation (2) to produce a combined standard uncertainty U_c. The final stage of the calculation involves using the coverage factor k=2 in Equation (3) to obtain the span uncertainty U_{exp}, which provides a 95% confidence level for the measured gauge block surface roughness value. This procedure ensures that the proposed non-contact measurement system has metrologically acceptable accuracy.

RESULT AND DISCUSSION

Light Direction Calibration

Calibrating the light direction emitted by LEDs determines the actual lighting characteristics of each light source used in a stereo photometric system. This process involves determining the primary direction of illumination (light vector), the location of the light source, and the degree of light dimming based on the beam's distance and direction. To obtain this data, a calibration pattern, such as a reflective sphere, is used (to accurately capture light reflections). The results of this process are used in lighting modelling to account for the actual effects of LED light on the object's surface. This calibration enables more accurate three-dimensional surface reconstruction by adjusting the lighting factors to reflect actual experimental conditions [14].

ISSN 2580-6424 (printed) | ISSN 2477-2399 (online)

Testing of Photometric Image Acquisition Function

Light direction calibration testing is carried out to ensure that the direction of light coming from the surface of the test object gauge block is known and to standardize lighting conditions. This test involves turning on one LED at a time, while the others are turned off. Each time a light is turned on, the camera captures a single image of the surface of a solid sphere as seen in Figure 5. These images are used to analyze intensity differences at each pixel caused by different light directions. This process is repeated six times (for each of the six light directions).

Using a reflective spherical pattern so that light reflection can be used to calculate the position of the light [14]. The purpose of calibration is to ensure that the position of the light source does not affect the results of the photo or observation. The light direction vector, as an image processing algorithm, requires information about the light source to calculate the surface normal and reconstruct the 3D profile of the object (gauge block). These six directions produce the lighting variations needed to form the surface profile.

Photometric Image Acquisition Function Testing

The photometric image acquisition function captures six images of the same object under different lighting directions, using a camera and a microcontroller-controlled lighting system. Six LEDs are mounted around the object and turned on one at a time. Each LED is turned on in turn, and once the lighting stabilizes, the camera captures an image and saves it in PNG format. Once the image capture is complete, the LEDs turn off, and the process continues with the next LED.

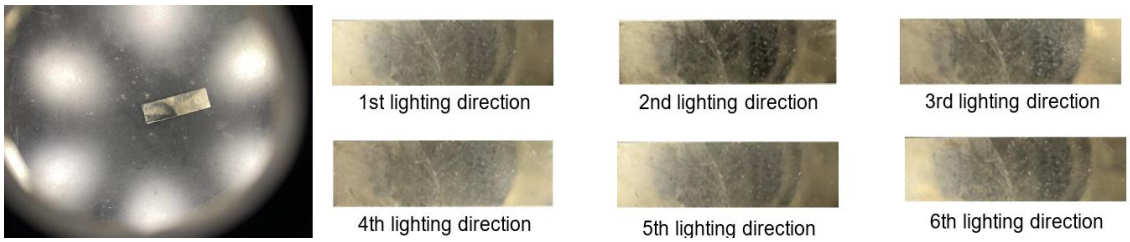

Figure 6. Results of image acquisition of the surface of the test object

The acquisition process was performed six times with different lighting conditions for each image capture. These images consist of six images. Each image is shown in Figure 6, which depicts the surface of a two-dimensional gauge block object with its shadow and light-reflection characteristics under six lighting sources. These six two-dimensional images were used in the photometric process to form a three-dimensional surface model.

Photometric Reconstruction Test Results

Photometric reconstruction testing involves reconstructing the surface shape of a three-dimensional object from a series of two-dimensional images. The system uses six images of the object, each taken under lighting from a different direction. By having at least three images with different lighting, the system can calculate the surface normal for each pixel. Using more than three images, such as six, aims to minimize noise. In Figure 7, you can see the results of the 3D reconstruction.

ISSN 2580-6424 (printed) | ISSN 2477-2399 (online)

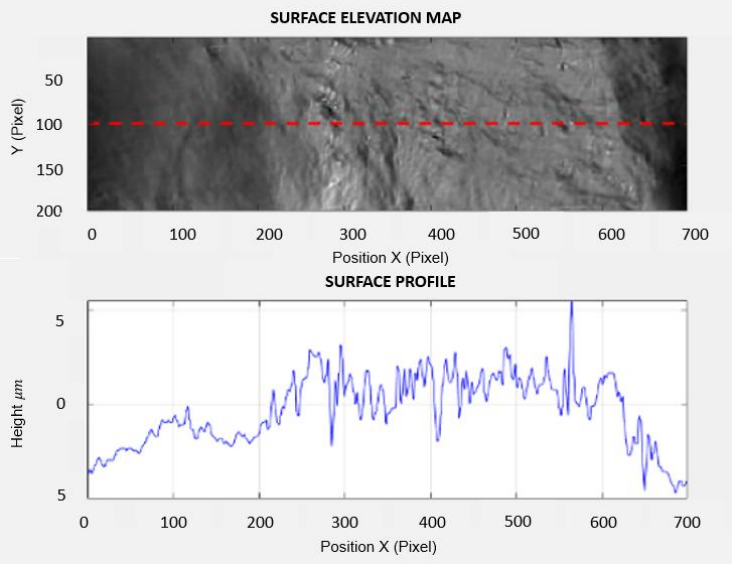

Figure 7. 3D reconstructed surface profile of the gauge block using six-light photometric stereo. The color bar represents the reconstructed surface height in micrometers (µm).

In Figure 8, the X, Y, and Z-axis graphs of the surface depth are shown, displaying the surface area (gauge block). The dotted red line indicates the selected surface profile path, and this graph shows surface height (in µm) versus X position (pixels) to calculate surface roughness parameters such as Ra, Rq, and Rz. This test uses the unbiased_ps_directional function, a Photometric Stereo algorithm for directional lighting. This function produces two main outputs: a depth matrix (z) representing the object's three-dimensional shape, and a surface normal matrix (N) containing surface information at each pixel.

Calibration Results of Class 0 Gauge Block

Table 2. Average Photometric Reconstruction Test of Class 0 Gauge Block

Nominal length of gauge block (mm)	Average Ra (µm)	Roughness Standard (µm)	Error (µm)	Uexp (µm)
1.01	1.5712	1.6	-0.029	0.09
1.02	1.9045	1.6	0.305	0.08
1.03	1.8945	1.6	0.295	0.08
1.04	1.7977	1.6	0.198	0.08
1.05	1.8623	1.6	0.262	0.08
1.06	1.8122	1.6	0.212	0.08
1.07	1.8122	1.6	0.212	0.08
1.08	2.1994	1.6	0.599	0.08
1.09	1.8945	1.6	0.295	0.08
1.10	1.7222	1.6	0.122	0.08

The table presents the surface roughness characterization results for ten gauge block samples with nominal lengths ranging from 1.01 mm to 1.10 mm. The measured average roughness (Ra) is the average of the peak height and depth of the 3D images showing significant variation across the specimens, with a minimum value of 1.5712 µm in the 1.01 mm block and a maximum value of 2.1994 µm in the 1.08 mm block. This measurement does not measure the depth of each peak and valley individually but is averaged via Matlab. Comparative analysis against the 1.6 µm reference standard revealed a dynamic error range, spanning from a negative deviation of -0.029 µm to a maximum positive error of 0.599 µm. Notably, the 1.06 mm and 1.07 mm blocks displayed identical roughness characteristics at 1.8122 µm. Furthermore, the expanded uncertainty (U_{exp}) remained constant at 0.08 µm throughout the dataset, confirming high measurement stability and reliability at a 95% confidence level.

ISSN 2580-6424 (printed) | ISSN 2477-2399 (online)

Table 3. Average Photometric Reconstruction Test of Class 1 Gauge Block

Nominal length of gauge block (mm)	Average Ra (µm)	Roughness Standard (µm)	Error (µm)	Uexp (µm)
1.01	2.6443	1.6	1.044	0.0924
1.02	2.1644	1.6	0.564	0.0924
1.03	2.7875	1.6	1.188	0.0924
1.04	2.6615	1.6	1.062	0.0924
1.05	2.7017	1.6	1.102	0.0924
1.06	2.6499	1.6	1.050	0.0924
1.07	2.6499	1.6	1.050	0.0924
1.08	2.3995	1.6	0.800	0.0924
1.09	2.5531	1.6	0.953	0.0924
1.10	2.4336	1.6	0.834	0.0924

Table 3 presents the surface roughness characterization data on ten gauge block samples with a nominal length range between 1.01 mm and 1.10 mm. Based on the measurement data, the average surface roughness Ra value shows fluctuations in each specimen, with the highest value of 2.7875 µm on the 1.03 mm nominal block and the lowest value of 2.1644 µm on the 1.02 mm block. All measurement results show a positive deviation or significant error relative to the roughness standard value of 1.6 µm, with an error range of 0.564 µm to 1.188 µm. The expanded uncertainty Uexp of 0.0924 µm at a 95% confidence level (k=2) indicates that the measurement process maintains stable precision, even though the surface roughness across all Class 1 samples lies methodologically above the reference threshold.

Previous research has shown that stereophotometry using three illuminations can measure the surface roughness of standard blocks better than stylus measurements, with an average error of 1.86–10.45 µm [2]. The results of the study using stereophotometry with six illuminations showed smaller errors than those of previous studies. The results of the standard block test had an average error of 0.3181 µm for a roughness value of 1.6 µm, while for the 3.2 µm standard block, it was -1.0718 µm. The average error for a Class 0 gauge block was -0.036 µm with an uncertainty of 0.08 µm, while the error for a Class 1 gauge block was -0.032 µm with an uncertainty of 0.0924 µm.

The accuracy and uncertainty of surface roughness measurements (Ra) showed a strong relationship with the use of a six-light-source configuration in the acquisition system. The scientific advantage of this configuration lies in the system's ability to reduce shadow effects that often distort the average roughness value on samples with irregular surface profiles. Test results show that the redundancy of information from six illumination directions can produce a more stable normal vector estimate, so that measurement deviations (errors) remain within the permissible metrological tolerance limits.

To minimize the observed systematic bias in Ra measurements, this study addresses key physical error sources by optimizing the central region of interest to suppress sub-pixel camera noise, applying a precise alignment calibration matrix for the six-LED setup, and introducing an enhanced mathematical reconstruction model to compensate for surface micro-shadowing effects.

A deeper interpretation of the results in Table 2 and Table 3 reveals distinct metrological behaviors between Class 0 and Class 1 gauge blocks. Class 0 and Class 1 naturally exhibit different R_a ranges due to their manufacturing tolerances and surface finishing standards, where Class 0 possesses a higher-grade surface finish with lower nominal roughness. The experimental data shows varying error values across different blocks, with the 1.08 mm block in Table 2 exhibiting the highest measurement error. Scientifically, this variance is primarily driven by localized surface conditions and material reflectivity rather than system instability. Smaller gauge blocks, such as the 1.08 mm specimen, are highly susceptible to micro-reflections and minor surface imperfections, which slightly distort the photometric stereo height reconstruction algorithm. However, despite these variations in absolute error

values, the expanded uncertainty values across all tests remain consistently low and uniform, indicating excellent measurement precision and high system repeatability.

Despite the error mitigation and optimization strategies implemented, certain residual errors inevitably persist due to combined physical and computational factors. First, the 8-bit image quantization during grayscale conversion introduces minor discretization errors in the pixel intensity matrices. Second, sub-pixel hardware limitations such as inherent camera sensor noise and slight mechanical misalignments in the LED positioning can cause subtle variations in the distance between the LEDs and the object surface, leading to non-uniform illumination intensity that propagates into the surface normal estimation. Furthermore, the highly reflective nature of the steel gauge blocks accentuates the localized specular reflections and micro-shadowing effects along the microscopic profiles. Collectively, these computational approximations, light source calibration uncertainties, and photometric stereo reconstruction algorithm limitations account for the remaining residual deviations observed between the measured Ra values and the reference standard values presented across both Table 2 and Table 3.However, despite the variations in absolute error values, the expanded uncertainty (Uexp) values across all tests remain consistently low and uniform. This behavior demonstrates that the developed six-lighting stereophotometry system possesses excellent measurement precision and high repeatability, confirming that the minor residual errors do not compromise the overall reliability of the system within permissible metrological limits.

To contextualize the performance and viability of the proposed six-light stereophotometry system, a brief comparison with established surface profilometry methods is essential. Traditional stylus profilometry provides direct mechanical measurements but introduces an inherent risk of scratching or damaging high-precision gauge blocks, while suffers from localized data tracking and low sampling speeds [2, 6]. To overcome these contact-based flaws, advanced optical methods such as confocal microscopy and coherence scanning interferometry (CSI) are widely employed in metrology laboratories. Both confocal microscopy and CSI offer superior axial resolutions down to the sub-nanometer scale; however, they require highly sophisticated optical paths, sensitive environmental vibration isolation, and significantly expensive hardware setups that limit their portability and widespread industrial shop-floor application.

In contrast, other conventional optical roughness measurement methods—such as basic laser scattering or standard three-light photometric stereo—frequently struggle with severe shadow distortions and spatial occlusions on reflective metal profiles [2, 7]. The proposed six-light stereophotometry system bridges this gap by offering a well-balanced metrological trade-off. While it operates with baseline computational approximations, it delivers a highly consistent expanded uncertainty of 0.08 µm. The primary advantage of this six-light framework lies in its significantly lower implementation cost, structural simplicity (utilizing a standard mobile image sensor and generic low-power LEDs), non-contact execution, and straightforward mathematical processing pipeline via MATLAB. This makes the developed system exceptionally cost-effective, easily implementable, and highly practical for rapid, non-destructive surface integrity screen testing directly within standard manufacturing lines

CONCLUSION

This study successfully developed a non-contact surface roughness measurement system for gauge blocks using a stereophotometry method equipped with an innovative six-light source configuration. The integration of six radial light sources effectively reduced shadow distortion and expanded illumination coverage, providing the necessary data redundancy to improve topographic reconstruction. Experimental evaluations on ten steel gauge block samples demonstrated that the system could measure the average surface roughness Ra within a range of 1.5712 µm to 2.1994 µm for Class 0 grades, and 2.1644 µm to 2.7875 µm for Class 1 grades. Through rigorous metrological analysis, the system yielded a consistent expanded uncertainty U_{exp} at a 95% confidence level (k=2), validating its high measurement repeatability and baseline stability.

Practically, this non-contact optical framework offers a robust alternative for precision inspection in automotive and advanced manufacturing industries, as it mitigates the risk of physical surface wear inherent to conventional stylus contact instruments. However, despite these advancements, residual systematic biases and measurement errors persist due to hardware and computational constraints. These

limitations primarily stem from 8-bit image quantization during grayscale conversion, sub-pixel camera sensor noise, and micro-shadowing effects aggravated by the highly reflective steel surface of the gauge blocks.

To address these remaining constraints, future work will focus on realistic optimizations. Key research directions include increasing the image bit depth to mitigate quantization errors, implementing high-precision light source calibration algorithms to correct sub-pixel illumination misalignments, and integrating advanced specular reflection masks within the photometric stereo pipeline to enhance measurement accuracy across highly reflective materials.

ACKNOWLEDGMENT

I would like to express my gratitude for the support of the Academy of Metrology and Instrumentation in developing this research.

REFERENCES

[1] Y. Cao, B. Ding, J. Chen, W. Liu, P. Guo, L. Huang, and J. Yang, "Photometric-stereo-based defect detection system for metal parts," Sensors, vol. 22, no. 21, 2022, doi: 10.3390/s22218374.

[2] T. Somthong and Q. Yang, "Average surface roughness evaluation using 3-source photometric stereo technique," International Journal of Metrology and Quality Engineering, vol. 7, no. 4, 2016, doi: 10.1051/ijmqe/2016024.

[3] I. Mujiarto and P. A. S., "Analisis nilai kekasaran dan kekerasan permukaan pada proses pemesinan," Jurnal Teknik Mesin, vol. 10, no. 2, 2022.

[4] L. Nielsen and M. Kiba, "Calibration of gauge block comparators," Measurement Science and Technology, vol. 30, no. 5, p. 055001, 2019, doi: 10.1088/1361-6501/ab07b4.

[5] R. M. Ratlalan and O. Valentine, "Simulasi hasil pengukuran dimensi gauge blocks menggunakan coordinate measuring machine type Crysta-Apex S," Jurnal Mekanova: Mekanikal, Inovasi dan Teknologi, vol. 10, no. 1, 2024.

[6] W. P. Syam, Metrologi Manufaktur: Pengukuran Geometri dan Analisis Ketidakpastian. Kudus: Penerbit Buku Ilmiah, 2018.

[7] L. Zhang and Z. Xu, "A review of photometric stereo techniques for surface roughness measurement," *Measurement Science and Technology*, vol. 31, no. 8, p. 085007, 2020, doi: 10.1088/1361-6501/ab816c.

[8] E. Juliastuti, I. Setiawan, V. Nadhira, and D. Kurniadi, "Photometric stereo method used for woven fabric density measurement based on 3D surface structure," Journal of Engineering and Technological Sciences, vol. 55, no. 6, pp. 659–668, 2023, doi: 10.5614/j.eng.technol.sci.2023.55.6.4.

[9] Geometrical Product Specifications (GPS) - Length standards - Gauge blocks, ISO Standard 3650, 1998.

[10] R. A. Dalimunthe, "Pemantau arus listrik berbasis alarm dengan sensor arus menggunakan mikrokontroler Arduino Uno," in Seminar Nasional Royal (SENAR), vol. 1, no. 1, pp. 333–338, 2018.

[11] A. Okur and V. S. Uygur, "A new application of surface roughness tester on fabrics," Journal of Textile and Apparel, vol. 18, no. 2, 2008.

[12] R. Leach, Good Practice Guide No. 37: The Measurement of Surface Texture Using Stylus Instruments. United Kingdom: National Physical Laboratory, 2001.

[13] A. Karami, "Image-based 3D metrology of non-collaborative surfaces," Ph.D. dissertation, Department of Engineering, University of Metrology, 2023.

[14] Y. Yang, E. Rigall, H. Fan, and J. Dong, "Point light measurement and calibration for photometric stereo," IEEE Transactions on Instrumentation and Measurement, vol. 73, pp. 1–11, 2023, doi: 10.1109/TIM.2023.3324512.

[15] Y. Quéau, B. Durix, T. Wu, D. Cremers, F. Lauze, and J.-D. Durou, "LED-based photometric stereo: Modeling, calibration and numerical solution," Journal of Mathematical Imaging and Vision, vol. 59, pp. 1–25, 2017 .

[16] R. F. V. Saracchini, J. Stolfi, and H. C. G. Leitao, "Shape reconstruction using a gauge-based photometric stereo method," in Proceedings of the XXXV Latin American Informatics Conference (CLEI), 2009.
[17] K. M. Ahmed, Y. A. AlTalhh, A. N. AlZamil, and N. M. AlQahtani, "Development of a novel interferometric system for short- and long-gauge block calibration," Measurement Science and Technology, vol. 35, no. 12, p. 126015, 2024, doi: 10.1088/1361-6501/ad6f12..
[18] T. Doiron and J. S. Beers, The Gauge Block Handbook (NIST Monograph 180). Washington, D.C.: National Institute of Standards and Technology, 2014.
[19] F. Wang, J. Ren, Guo, H. Ren, and B. Shi, "DiLiGenT-Pi: Photometric stereo for planar surfaces with rich details—benchmark dataset and beyond," in Proceedings of the IEEE/CVF International Conference on Computer Vision, 2023, pp. 9477–9487.
[20] J. Yu, R. Wang, X. Liu, J. Tong, J. Xi, Q. Tang, and L. Cao, "Accuracy improvements of near-field photometric stereo via light source calibration," Optics Express, vol. 33, no. 6, pp. 14207–14220, 2025, doi: 10.1364/OE.541203.
[21] C. Hernández, G. Vogiatzis, and R. Cipolla, "Multiview photometric stereo," IEEE Transactions on Pattern Analysis and Machine Intelligence, vol. 30, no. 3, pp. 548–554, 2008, doi: 10.1109/TPAMI.2007.70796.
[22] C. Moler and J. Little, "A history of MATLAB," Proceedings of the ACM on Programming Languages, vol. 4, no. HOPL, pp. 1–67, 2020, doi: 10.1145/3386331.
[23] Á. Loránd and Á. Drégelyi-Kiss, "Influence of surface roughness on the accuracy of dimensional measurements in X-ray computed tomography (CT): A study on 3D-printed workpieces," Advances in Science and Technology, vol. 165, pp. 169–177, 2025, doi: 10.4028/p-47z8v1.
[24] S. Riadi, S. Gunawan, and H. Iskandar, "Influence of indium tin oxide (ITO) poling temperature in vacuum on surface roughness of polyvinylidene fluoride (PVDF) film," Jurnal Polimesin, vol. 21, no. 6, pp. 2023–2032, 2023.
[25] K. Stępień, J. Świderski, and W. Makieła, "The importance of measurement uncertainty during gauge block calibration in determining compliance with specifications," Measurement, vol. 241, p. 115602, 2025.
[26] L. Shi, H. Zhang, and H. Li, "A comprehensive review of photometric stereo techniques," Computer Graphics Forum, vol. 39, no. 4, pp. 1–35, 2020.
[27] H. Dow, M. Perry, S. Pennada, R. Lunn, and S. Pytharouli, "3D reconstruction and measurement of concrete spalling using near-field photometric stereo and YOLOv8," Automation in Construction, vol. 166, p. 105633, 2024, doi: 10.1016/j.autcon.2024.105633.
[28] R. J. Woodham, "Photometric method for determining surface orientation from multiple images," Optical Engineering, vol. 19, no. 1, pp. 139–144, 1980.
[29] F. Lian, Q. Tan, and S. Liu, "Block thickness measurement using structured light vision," International Journal of Pattern Recognition and Artificial Intelligence, vol. 33, no. 1, pp. 1–15, 2019.
[30] Ministry of Trade of the Republic of Indonesia, "Minister of Trade Regulation No. 52: Legal metrology measurement standard," JDIH Kemendag, 2019.